

# The Effect of New Formulas for Lean Body Mass on Lean-Body-Mass–Normalized SUV in Oncologic $^{18}\text{F}$ -FDG PET/CT

Trygve Halsne<sup>1</sup>, Ebba Glørsen Müller<sup>2</sup>, Ann-Eli Spiten<sup>2</sup>, Alexander Gul Sherwani<sup>2</sup>, Lars Tore Gyland Mikalsen<sup>1</sup>, Mona-Elisabeth Revheim<sup>2,3</sup>, and Caroline Stokke<sup>1,4</sup>

<sup>1</sup>Department of Diagnostic Physics, Oslo University Hospital, Oslo, Norway; <sup>2</sup>Department of Nuclear Medicine, Oslo University Hospital, Oslo, Norway; <sup>3</sup>Institute of Clinical Medicine, University of Oslo, Oslo, Norway; and <sup>4</sup>Department of Life Sciences and Health, Oslo Metropolitan University, Oslo, Norway

Because of better precision and intercompatibility, the use of lean body mass (LBM) as a mass estimate in the calculation of SUV (SUL) has become more common in research and clinical studies today. Thus, the equations deciding this quantity must be those that best represent the actual body composition. **Methods:** LBM was calculated for 44 patients examined with  $^{18}\text{F}$ -FDG PET/CT scans by means of the sex-specific predictive equations of James and Janmahasatian, and the results were validated using a CT-based method that makes use of the eyes-to-thighs CT component of the PET/CT acquisition and segments the voxels according to Hounsfield units. Intraclass correlation coefficients and Bland–Altman plots were used to assess agreement between the various methods. **Results:** A mean difference of 6.3 kg (limits of agreement, –15.1 to 2.5 kg) between  $\text{LBM}_{\text{James}}$  and  $\text{LBM}_{\text{CT1}}$  was found. This difference was higher than the 3.8-kg difference observed between  $\text{LBM}_{\text{Jan}}$  and  $\text{LBM}_{\text{CT1}}$  (limits of agreement, –12.5 to 4.9 kg). In addition,  $\text{LBM}_{\text{Jan}}$  had a higher intraclass correlation coefficient with  $\text{LBM}_{\text{CT1}}$  (0.87; 95% confidence interval, 0.60–0.94) than with  $\text{LBM}_{\text{James}}$  (0.77; 95% confidence interval, 0.11–0.91). Thus, we obtained better agreement between  $\text{LBM}_{\text{Jan}}$  and  $\text{LBM}_{\text{CT1}}$ . Although there were exceptions, the overall effect on SUL was that  $\text{SUL}_{\text{James}}$  was greater than  $\text{SUL}_{\text{Jan}}$ . **Conclusion:** We have verified the reliability of the suggested  $\text{LBM}_{\text{Jan}}$  formulas with a CT-derived reference standard. Compared with the more traditional and available set of  $\text{LBM}_{\text{James}}$  equations, the  $\text{LBM}_{\text{Jan}}$  formulas tend to yield better agreement.

**Key Words:** standardized uptake value; lean body mass; PET/CT; CT-based segmentation

J Nucl Med Technol 2018; 46:253–259

DOI: 10.2967/jnm.117.204586

The number of PET/CT investigations has increased for various oncology applications, including lung cancer investigations. PET allows noninvasive quantitative assessment of biochemical and functional processes, and SUV is a common quantitative measure used in clinical studies and

research. In general, SUV is defined as the ratio of the radioactive concentration measured in an area of interest to the injected activity divided by a mass estimate for the total distribution volume of the injected activity:

$$\text{SUV} = \frac{c_{\text{AOI}}}{A_{\text{inj}}} m_e, \quad \text{Eq. 1}$$

where  $c_{\text{AOI}}$  is the concentration in an area of interest,  $A_{\text{inj}}$  is the injected activity corrected for decay, and  $m_e$  is a mass estimate for the total distribution volume of the activity. In clinical practice and tradition, body weight is often used as a mass estimate. Thus, the value is denoted as SUV, which is made unitless assuming that the patient has a homogeneous mass density of  $1 \frac{\text{g}}{\text{mL}}$ .

In  $^{18}\text{F}$ -FDG PET/CT, several studies have reported a strong correlation between SUV and body weight due to the lack of body composition and body size information (1–3). It is common knowledge that adipose tissue metabolizes far less  $^{18}\text{F}$ -FDG than do other tissues in the fasting state and, consequently, that the SUVs of adipose patients may differ from those of lean patients for the same tumor uptake (1,2,4). Therefore, alternative methods that use lean body mass (LBM) as a mass estimate in Equation 1 have been proposed. SUV using LBM as a mass estimate is referred to as SUL.

LBM consists of the body cell mass and the nonfatty intercellular connective tissue, such as tendons and ligaments (5). Traditionally, body fat was quantified by skin-fold measurements and bioelectrical impedance analysis, but today, noninvasive imaging techniques are considered the gold standard for body composition and anthropometric analysis (6). CT, MRI, and dual-energy x-ray absorptiometry are the most frequently used modalities for this purpose (7).

Because CT-based methods are currently not applicable for clinical examinations, LBM is calculated from predictive equations by means of parameters such as sex, height, and body weight (8). A common set of equations in modern scanners is referred to as the James equations. They are based on skin-fold measurements and calculate LBM as

$$\text{LBM}_{\text{James}} = \begin{cases} 1.1 bw - 128 \left(\frac{bw}{h}\right)^2 & \text{for men} \\ 1.07 bw - 148 \left(\frac{bw}{h}\right)^2 & \text{for women} \end{cases}, \quad \text{Eq. 2}$$

Received Nov. 8, 2017; revision accepted Dec. 24, 2017.

For correspondence or reprints contact: Trygve Halsne, Department of Ocean and Ice, Norwegian Meteorological Institute, Henrik Mohns Plass 1, 0313 Oslo, Norway.

E-mail: trygve.halsne@met.no

Published online Mar. 29, 2018.

COPYRIGHT © 2018 by the Society of Nuclear Medicine and Molecular Imaging.

where  $bw$  is body weight and  $h$  height (9). The James formalism has a well-known weakness resulting in a negative correlation with body mass index (BMI), defined as  $bw/h^2$  (10). Janmahasatian et al. (11) used another approach and developed predictive equations based on bioelectrical impedance analysis. In this method, the total-body water is assumed to be a constant fraction of fat-free mass, such that fat-free mass can be estimated from the ratio of total-body water to the constant water fraction from the impedance index. Fat-free mass does not include fat in cell membranes, making fat-free mass slightly different from LBM (5), but for simplicity we denote fat-free mass as LBM in the set of equations. The equations, which Janmahasatian et al. verified with dual-energy x-ray absorptiometry measurements, read

$$LBM_{jan} = \begin{cases} \frac{9.27 \times 10^3 bw}{6.68 \times 10^3 + 216 BMI} & \text{for men} \\ \frac{9.27 \times 10^3 bw}{8.78 \times 10^3 + 244 BMI} & \text{for women} \end{cases} \quad \text{Eq. 3}$$

In general, basing predictive equations on the present demography is complicated by, for example, ethnic and epoch differences (12). Hence, efforts have been made to extract the LBM for SUL calculations by using the already-existing attenuation-correction CT component of the PET/CT examination (13).

Chan (13) developed a technique to estimate LBM from a limited-field-of-view CT scan and found that the CT-computed LBM was more accurate than results obtained from predictive equations. The reliability of his method was confirmed in a later study that compared the results with 5 predictive equations (14). Another group found substantial discrepancies between individual LBMs from CT scans and predictive equations by comparing 4 sets of predictive equations with CT-computed LBM using a built-in software package from Siemens to extract adipose tissue and adipose tissue-free body mass (15). The CT-based method developed by Hamil et al. has several similarities to the method developed by Chan but differs in some respects, such as the introduction of a skin component to address partial-volume effects.

This study aimed to compare SULs from the 2 sets of predictive equations,  $LBM_{james}$  and  $LBM_{jan}$  (i.e., Eqs. 2 and 3), with CT-based SUL methods by means of statistical analysis.  $LBM_{jan}$ , which constitutes the new European Association of Nuclear Medicine guideline for LBM calculations (16), has not, to our knowledge, been previously compared with and validated against a CT-based method for LBM.

## MATERIALS AND METHODS

### Patient Population

In total, 44 patients were included in the present prospective study. Consecutive patients referred for lung cancer assessment were asked to participate. Their characteristics are listed in Table 1. The institutional review board approved this study, and all subjects signed a written informed consent form. The patients were selected according to their BMI to obtain approximately

**TABLE 1**  
Patient Characteristics

Characteristic	BMI range		
	18.5–24.9	25.0–29.9	30.0–∞
Subjects (n)	15	16	13
Measured BMI	22.4 ± 1.6	27.3 ± 1.4	32.7 ± 4.1
Height (m)	1.66 ± 0.06	1.71 ± 0.07	1.73 ± 0.10
Weight (kg)	62.2 ± 6.1	80.1 ± 9.0	98.0 ± 8.8
Sex (n)			
Male	5	9	9
Female	10	7	4

15 subjects in each of 3 intervals: 18.5–24.9, 25.0–29.9, and 30.0–∞. Exclusion criteria were patients with large metallic implants, proven diabetes, or a blood glucose level higher than 8.3 mmol/L (16).

### PET/CT Acquisition Protocols

For the PET/CT image acquisition, we used a Siemens Biograph 64. The patients fasted for at least 6 h before undergoing imaging. The amount of injected  $^{18}\text{F}$ -FDG was based on the patient's age and body weight (17). Sixty minutes after injection, the patients were scanned. The CT acquisition parameters were 120 kV, 3.0-mm slice thickness, 50 mAs, and a 1.35 pitch using a B31f kernel for the reconstructed images. In the PET protocol, we scanned at a rate of 3 min/bed position using ordered-subsets expectation maximization with 4 iterations and 8 subsets, creating a  $168 \times 168$  matrix smoothed with a 5.0-mm gaussian filter.

### Area-of-Interest Definition in Determination of SUV

The  $SUV_{max}$  and  $SUV_{peak}$  of the lesions, and the  $SUV_{mean}$  and SD of the liver, were measured and registered using a Siemens SyngoVia workstation (version VB10A).  $SUV_{max}$  and  $SUV_{peak}$  were measured manually by placing a volume of interest over target lesions.  $SUV_{peak}$  was defined as a volume of 1 cm<sup>3</sup> around the site of maximum uptake. All chosen lesions were evaluated as pathologic by a nuclear medicine physician. Liver background uptake was measured by placing a 3-cm region of interest in the right liver lobe according to PERCIST (4). Cross-sectional regions were displayed in axial, sagittal, and coronal projections in such a way that no hypermetabolic uptake was included in the reference regions. Target lesions were defined as tumor in the lung parenchyma (for 39 patients), and if there was more than one, we included that with the highest  $^{18}\text{F}$ -FDG uptake. In the 3 patients who showed no evidence of a lung tumor, we applied the volume of interest over the most hypermetabolic mediastinal or hilar lymph node. In 1 patient, we placed a volume of interest over hypermetabolic pleura, as this was the only finding. In 1 other patient, no volume of interest was applied, as there was no evidence of a lung tumor, hypermetabolic pleura, or a hypermetabolic lymph node.

### Data Analysis

$LBM_{james}$  (Eq. 2) is calculated using  $bw$  in kilograms and  $h$  in centimeters. For the calculation of  $LBM_{jan}$ ,  $h$  is in meters for the computation of BMI.

The CT-based method developed by Hamil et al. (18) makes use of the eyes-to-thighs CT portion of the PET/CT acquisition. The method is based on estimates of lean tissue, fat, and bone from counting all voxels in a characteristic range of Hounsfield units, multiplied by voxel size and a characteristic density. An

example of how the segmentation process takes place in a single axial image is shown in Figure 1. The LBM formalisms read

$$\text{LBM}_{\text{CT1}} = bw \left( \frac{\text{lean} + \text{bone}}{\text{lean} + \text{fat} + \text{bone}} \right) \quad \text{Eq. 4}$$

$$\text{LBM}_{\text{CT2}} = m_1 + (bw - m_2) \frac{\text{lean} + k_{\text{fat}} \times \text{fat}}{\text{lean} + \text{fat} + \text{bone}}, \quad \text{Eq. 5}$$

where  $m_1$  and  $m_2$  represent the brain and head mass, respectively, in kilograms;  $k_{\text{fat}}$  is a proportionality constant representing the relative uptake in fatty tissue to lean tissues; and the terms *lean*, *fat*, and *bone* represent the weight, in kilograms, of these 3 tissue types. In contrast to the more intuitive  $\text{LBM}_{\text{CT1}}$ ,  $\text{LBM}_{\text{CT2}}$  is meant to model the body's processing of  $^{18}\text{F}$ -FDG. Because of the limited CT field of view,  $m_1$ ,  $m_2$ , and  $k_{\text{fat}}$  are estimated parameters.

Both the predictive equations and the CT-based method were implemented using the Python programming language (Python Software Foundation, version 2.7) along with the statistical analysis. The implementation of the CT-based method was verified by a head-to-toe CT scan in which the entire patient was within the field of view, and the patient's body weight was compared in the same way as previously published (18), where

$$\text{CT}_{\text{me}} = \text{lean} + \text{fat} + \text{bone}. \quad \text{Eq. 6}$$

$\text{CT}_{\text{me}}$  denotes mass estimate from CT. The difference between actual body weight and  $\text{CT}_{\text{me}}$  was on the order of a tenth of a kilogram, which is considered a satisfying result that implies correct implementation of the method.

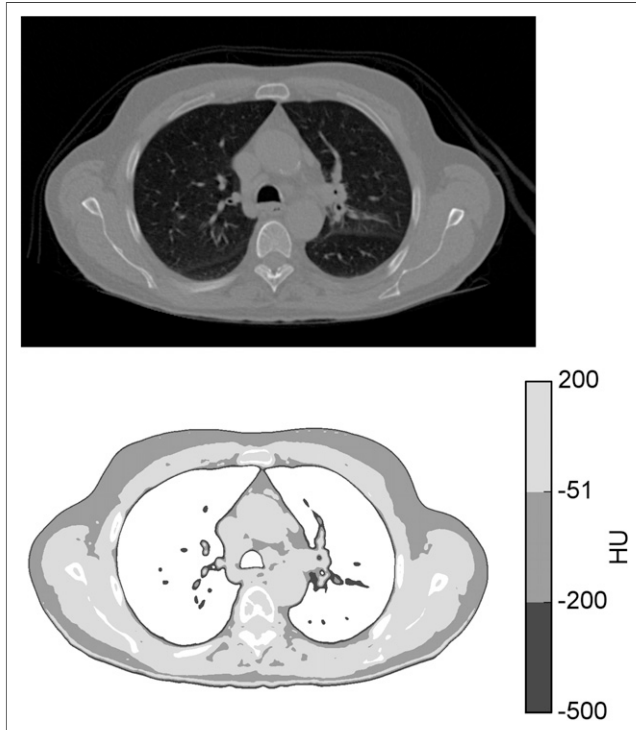


**FIGURE 1.** Tissue segmentation in accordance with CT-based method described by Hamil et al. (18). (Top) CT thorax image in axial projection. (Bottom) Regions segmented as skin, fat, and LBM in Hounsfield units (HU) of -500 to -201, -200 to -51, and -50 to 200, respectively.

All SULs are calculated as

$$\text{SUL}_i = \frac{\text{SUV}_{bw}}{bw} \text{LBM}_i \quad \text{Eq. 7}$$

where subscript  $i$  denotes the 4 various LBM calculations from Equations 2–5.

### Statistical Analysis

For continuous variables, mean  $\pm$  SD is reported. The Bland–Altman analysis was used to investigate absolute differences between two methods (19). The average difference (bias) and the limits of agreement, between which 95% of all comparisons lie, are reported. In addition, intraclass correlation coefficient (ICC) with 95% confidence interval was used to assess agreement among different types of measurements (20). In all cases,  $\text{LBM}_{\text{CT1}}$  was used as the reference standard. The normality of distributions was graphically checked, and 95% confidence intervals were used.

Pearson correlation coefficients ( $r$ ) and regression lines were computed for liver SUL versus BMI, and tumor  $\text{SUL}_{\text{max}}$  and  $\text{SUL}_{\text{peak}}$  are presented using bar plots. A paired-sample  $t$  test was used to compare the differences in tumor-value results based on predictive equations.

### RESULTS

Figure 2 presents the various LBM methods compared by means of Bland–Altman plots. The mean difference and limits of agreement are computed for both sexes together.

We found good agreement between  $\text{LBM}_{\text{james}}$  and  $\text{LBM}_{\text{jan}}$ , especially for men (Fig. 2A). For women,  $\text{LBM}_{\text{james}}$  introduced a systematic overprediction compared with  $\text{LBM}_{\text{jan}}$  ( $\sim 5$  kg). The negative outlier resulted from a female patient with a BMI of 42.

We observed a bias in the direction of LBM overestimation for both  $\text{LBM}_{\text{james}}$  and  $\text{LBM}_{\text{jan}}$  when compared directly with  $\text{LBM}_{\text{CT1}}$  (6.3 and 3.8 kg, respectively) (Figs. 2C and 2D). The limits of agreement were approximately the same (95% confidence interval, 8.8 and 8.7 kg for  $\text{LBM}_{\text{james}}$  and  $\text{LBM}_{\text{jan}}$ , respectively), showing that the interpatient variation was about the same. The ICCs shown in Table 2 yielded similar results, with an ICC of 0.87 (95% confidence interval, 0.60–0.94) for  $\text{LBM}_{\text{jan}}$  and 0.77 (95% confidence interval, 0.11–0.91) for  $\text{LBM}_{\text{james}}$ .

The impact of each method on measured tumor SUL was investigated for each patient individually. The tumor  $\text{SUL}_{\text{peak}}$  and  $\text{SUL}_{\text{max}}$ , computed for all patients using the 3 LBM formulations in Equations 2–4, are shown in Figure 3.

The overall trend was for  $\text{SUL}_{\text{james}}$  to be greater than  $\text{SUL}_{\text{jan}}$ , which again tended to be greater than our chosen gold standard method,  $\text{SUL}_{\text{CT1}}$ . There were, however, exceptions. The interpatient variation was greater than the method differences. Compared with  $\text{SUL}_{\text{jan}}$ ,  $\text{SUL}_{\text{james}}$  gave a median tumor  $\text{SUL}_{\text{max}}$  of 0.64 (range, 0.0–1.3) and a median tumor  $\text{SUL}_{\text{peak}}$  of 0.58 (range, 0.0–1.2). No significant differences between  $\text{SUL}_{\text{jan}}$  and  $\text{SUL}_{\text{james}}$  in relation to  $\text{SUL}_{\text{CT1}}$  were found ( $P > 0.05$  for peak values and maximum values).

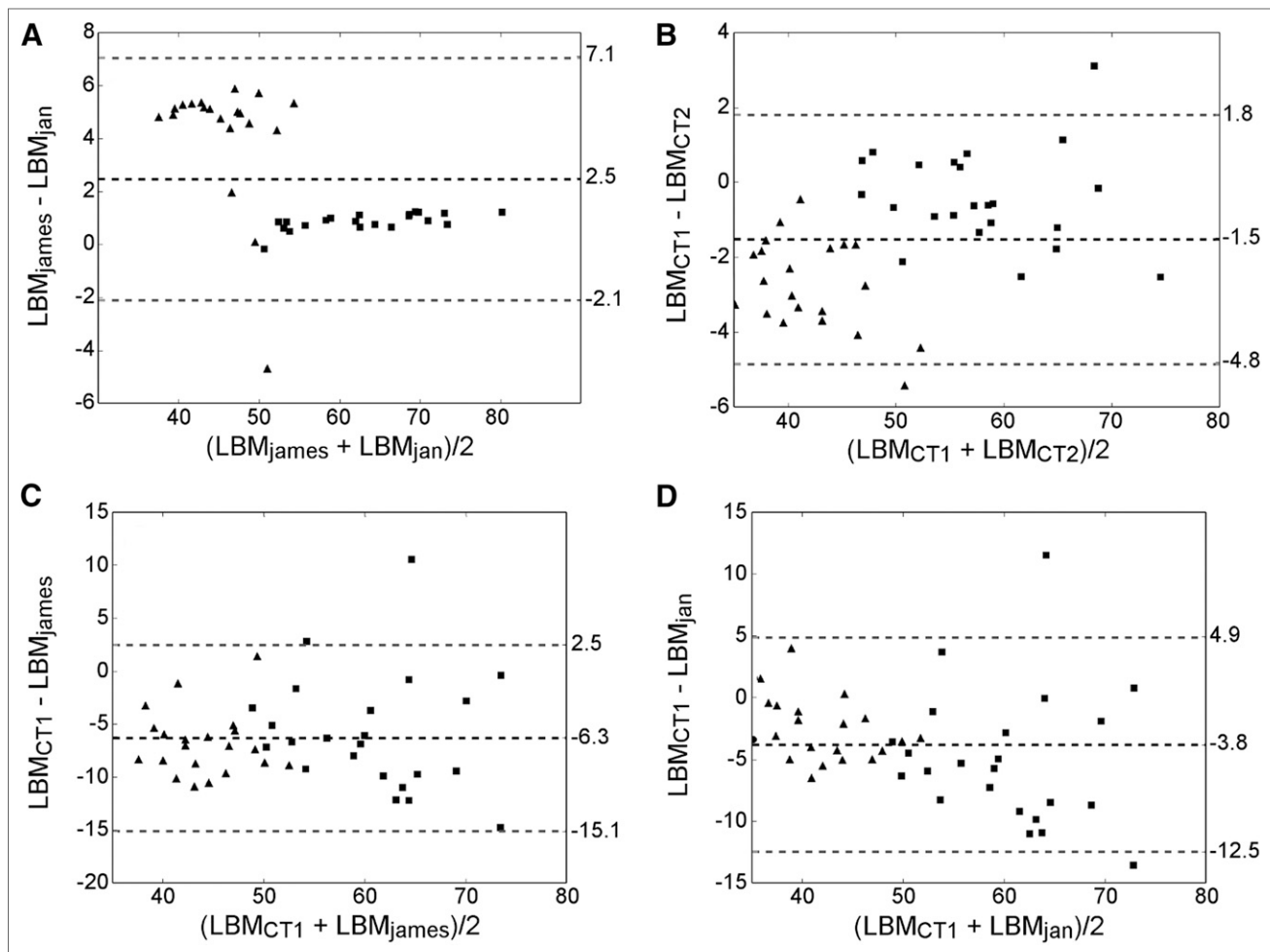


**FIGURE 2.** Bland–Altman plots illustrating differences between LBM<sub>james</sub> and LBM<sub>jan</sub> (A), LBM<sub>CT1</sub> and LBM<sub>CT2</sub> (B), LBM<sub>CT1</sub> and LBM<sub>james</sub> (C), and LBM<sub>CT1</sub> and LBM<sub>jan</sub> (D). Dashed black lines denote mean difference, whereas gray dashed lines denote limits of agreement. Squares and triangles denote male and female patients, respectively.

In Figure 4, liver SUL and SUV<sub>mean</sub> are plotted against BMI together with an associated linear regression line to show the impact of BMI on the computed uptake values. The range of mean liver SUV, 1.70–2.87, was within that specified in the European Association of Nuclear Medicine guidelines (16).

Two methods for CT-derived LBM were implemented. These were compared, and the results (Fig. 2B; Table 2) showed only a modest disagreement: an ICC of 0.98 (95%

confidence interval, 0.89–0.99), bias of –1.5 kg, and a limit of agreement of –4.8 to 1.8 kg.

Our dataset included 4 patients with metallic implants: 3 with a hip replacement and one with a pacemaker. In the case of the pacemaker, the difference after removing 6 partially distorted axial planes in the middle of the mediastinum was 0.1% for LBM<sub>CT1</sub> and therefore of little concern. In the case of the hip replacements, the distortion did not affect the entire image, but we chose to exclude the axial planes of the CT series that showed the metallic implant. For these patients, the largest observed difference in LBM<sub>CT1</sub> was 2.4%, with 48.1 versus 49.2 kg, and was considered negligible.

## DISCUSSION

Both LBM<sub>james</sub> and LBM<sub>jan</sub> use different equations for male and female patients. Our results showed a systematic difference between LBM<sub>james</sub> and LBM<sub>jan</sub> for the female patients, whereas the results for the male patients were in relatively good correspondence. Consequently, changing

**TABLE 2**  
ICCs Using LBM<sub>CT1</sub> as Reference

Method	LBM	ICC	95% confidence interval	P
LBM <sub>james</sub>	55.8 ± 10.2	0.77	0.11–0.91	< 0.001
LBM <sub>jan</sub>	53.3 ± 11.7	0.87	0.60–0.94	< 0.001
LBM <sub>CT2</sub>	51.0 ± 9.6	0.98	0.89–0.99	< 0.001
LBM <sub>CT1</sub>	49.5 ± 10.4	1		—

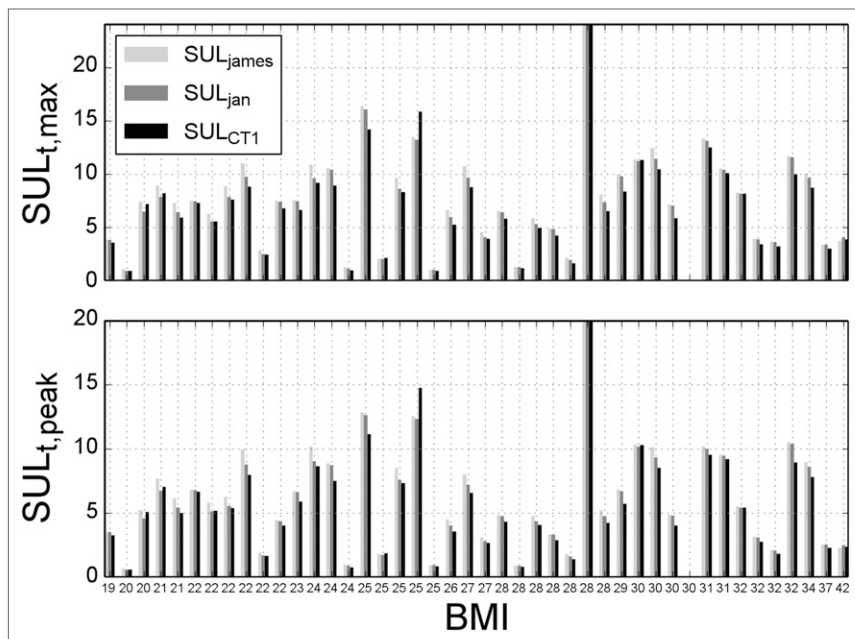


**FIGURE 3.** Bar plots showing how variations in LBM calculation can affect maximum and peak SUL for individual tumors. SUL of a single tumor is given for each patient, with patients being sorted by increasing BMI.

from  $LBM_{james}$  to  $LBM_{jan}$  will most strongly affect female patients.

It is to be expected that patients with a very high BMI show up as outliers in the results when  $LBM_{james}$  and  $LBM_{jan}$  are compared directly. This is a consequence of the James equations, which have a known negative bias for high-BMI patients, originating from the parabolic nature of the equations (10). The female equation obtains its maximum when BMI is approximately 37. After that point, LBM will decrease with increasing BMI. Such is also the case for the male equation, but with a higher maximum, at a BMI of about 43. In their paper, Tahari et al. (10) argue for the replacement of  $LBM_{james}$  with  $LBM_{jan}$  because of the significant difference for high-BMI patients, but their lack of quantitative comparison between  $LBM_{james}$  and  $LBM_{jan}$  does not reveal the method difference in the lower-BMI regions. Although the Pearson correlation coefficients for SUV and SUL versus body weight were lower for  $LBM_{jan}$  than for  $LBM_{james}$ ,  $LBM_{jan}$  was not validated as a reliable measure for true LBM.

We observed a bias in the direction of LBM overestimation for both  $LBM_{james}$  and  $LBM_{jan}$  compared with  $LBM_{CT1}$  (6.3 kg and 3.8 kg, respectively). The lower bias for  $LBM_{jan}$  makes this the preferred method. The ICCs shown in Table 2 yield the overall same results as the Bland–Altman analysis; that is,  $LBM_{jan}$  has better agreement with  $LBM_{CT1}$  than  $LBM_{james}$ . The ICC of 0.87 for  $LBM_{jan}$  shows a better extent of correspondence between the methods than does the ICC for  $LBM_{james}$ , at 0.77.

Decazes et al. (14) used the same statistical techniques, that is, Bland–Altman plots and ICCs, to verify Chan's CT models (13) but seemingly implemented  $LBM_{james}$  incorrectly

using 120 instead of 128 in the second term for males and  $h$  instead of  $bw$  in the first term for females. Hence, their results may not be comparable. Both their comparison with other equation-based methods and the comparisons made by Erselcan et al. (12) find discrepancies with a reference standard, using dual-energy x-ray absorptiometry in the latter case. The general trend is that if the mean values from a Bland–Altman analysis are smaller, those come at the cost of an overestimation for the leanest patients and an underestimation for the most adipose patients, leaving us with a biased function. In cases without a biased function, the limits of agreement are about the same size as for  $LBM_{james}$  in these studies.

The positive outlier in Figures 2B–2D was due to a subject with a large muscular mass with low percentage of fat. It is to be expected that predictive equations using BMI as a measure of

fat content have difficulty estimating LBM in this type of patient.

We chose the  $LBM_{CT}$  methods as the gold standard in our analysis based on multiple studies (2,6,13,14), although there are several variations within these CT-based methods, including differences in Hounsfield unit range and tissue density. Besides these differences, Decazes et al. (14) argued that the nonuniform tissue distribution in Chan's method reflects reality better than the uniform distribution of fat, lean, and bone used in  $LBM_{CT1}$ . On the other hand,  $LBM_{CT2}$  is meant to consider the case of nonuniform distribution, introducing tracer uptake in fat and differences in fat content in the head. There are differences in LBM calculations from the various CT methods, although these differences are smaller than those obtained with the predictive equations. Hence, we included the  $LBM_{CT2}$  method in our study and observed a good correspondence between the 2 CT-based methods. In comparison,  $LBM_{CT2}$  also tells us something about the uncertainty of the limited field of view in  $LBM_{CT1}$ . Less bias and high ICCs,  $-1.5$  kg and 0.98 (95% confidence interval, 0.89–0.99), respectively, confirm the robustness of the latter method. Because  $LBM_{CT2}$  is not considered validated, according to the author (18), we performed the SUL analysis using CT1 as the reference.

Metallic implants are a challenge when CT is used for LBM. An increase in BMI also tends to correlate with the number of people having metallic implants as a result of overuse injuries. But on the basis of our experience, the CT-based methods yield more consistent results than the predictive equations for this group. In accordance with Hamill et al. (18), the change was smaller for  $LBM_{CT2}$ . This finding also corresponds to earlier studies that found CT

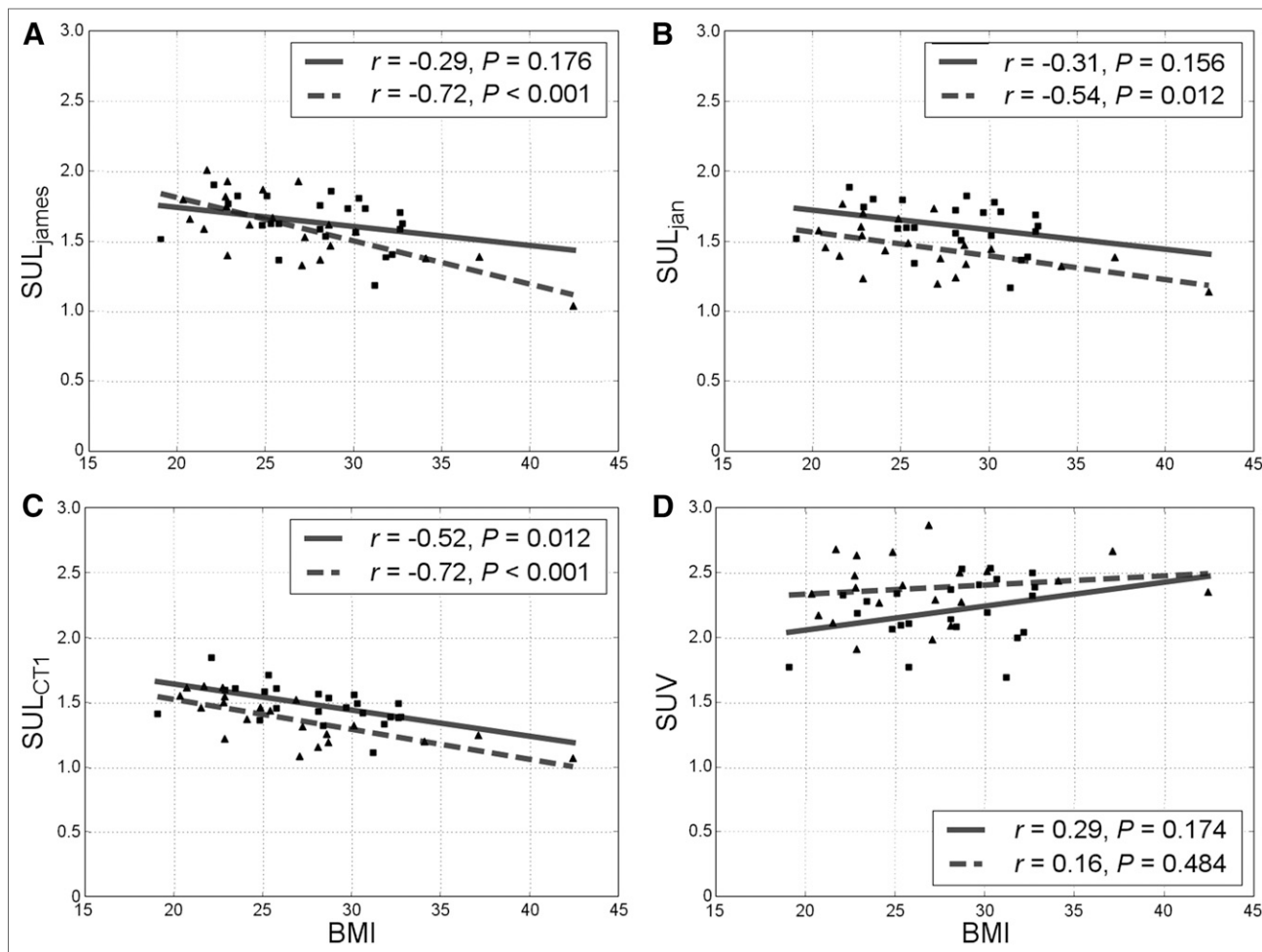


**FIGURE 4.** Liver SUL vs. BMI for  $SUL_{james}$  (A),  $SUL_{jan}$  (B),  $SUL_{CT1}$  (C), and BMI (D). Squares and triangles denote male and female patients, respectively, with associated solid regression lines.

methods to agree well across variations in field of view (14). Another challenge for CT-based methods is the presence of large-volume ascites, pleural effusions, or soft-tissue edema. Here, one could experience a relative bias toward overestimation of LBM because these regions will falsely be characterized as lean tissue while usually taking up no  $^{18}F$ -FDG. That said, the predictive equations using such parameters as body weight and height would also struggle with these types of volumes. In our patient population, none of the above-mentioned volumes were present.

The results from our SUL computations in Figure 3 underscore the result from Figure 2, that  $LBM_{james}$  in general overpredicts LBM, compared with  $LBM_{jan}$  and  $LBM_{CT1}$ . The only case in which the opposite is evident in Figure 3 (a patient with a BMI of 25) is one with  $SUL_{max}$  and  $SUL_{peak}$  higher for  $SUL_{CT1}$  than for  $SUL_{james}$  and  $SUL_{jan}$ . This patient is the same as referred to earlier: the muscular subject with a low percentage of fat compared with the others. None of these patients would be diagnosed differently based on the results from the 3 LBM formulations,

since the diagnosis often is based on the overall evaluation and not on SUL alone. However, it is obvious that a more precise SUL will contribute to better patient diagnostics and treatment evaluation in the long term.

Figure 4 shows a classic way to evaluate results by plotting BMI versus liver SUL with associated regression lines, which ideally should be uncorrelated. In contrast to Tahari et al. (10), we systematically found a negative correlation for female patients in both  $SUL_{james}$  and  $SUL_{jan}$  (Figs. 4A and 4B). That said, the overall results were about the same. The number of patients in the compared study was significantly higher (i.e., 1,033 vs. 44), with emphasis on patients with a BMI of less than 30. However, the lack of a direct quantitative comparison between the methods makes this study important in terms of validation.

## CONCLUSION

We have verified the reliability of the suggested  $LBM_{jan}$  formulas against a CT-derived reference standard.  $LBM_{jan}$  tended to yield better agreement with the CT-based method, especially for female patients, than did  $LBM_{james}$ , which is

the most available SUL formulation used today. It is anticipated that the new LBM-adjusted SUV, which is also recommended in version 2.0 of the European Association of Nuclear Medicine guidelines for tumor imaging, can improve the accuracy and consistency of SUL calculations in research and clinical practice.

## DISCLOSURE

No potential conflict of interest relevant to this article was reported.

## ACKNOWLEDGMENT

We greatly appreciate the assistance of the nuclear medicine technicians at Rikshospitalet, Oslo University Hospital.

## REFERENCES

- Zasadny KR, Wahl RL. Standardized uptake value of normal tissue at PET with 2-[fluorine-18]-fluoro-2-deoxy-D-glucose: variations with body weight and a method for correction. *Radiology*. 1993;189:847–850.
- Kim CK, Gupta NC, Chandamouli B, Alavi A. Standardized uptake values of FDG: body surface area correction is preferable to body weight correction. *J Nucl Med*. 1994;35:164–167.
- Sugawara Y, Zasadny ZK, Neuhoff AW, Wahl RL. Reevaluation of the standardized uptake value for FDG: variations with body weight and methods for correction. *Radiology*. 1999;213:521–525.
- Wahl RL, Jacene H, Kasamon Y, Lodge MA. From RECIST to PERCIST: evolving considerations for PET response criteria in solid tumors. *J Nucl Med*. 2009;50(suppl):122S–150S.
- Roubenoff R, Kehayias JJ. The meaning and measurement of lean body mass. *Nutr Rev*. 1991;49:163–175.
- Heymsfield SB, Gonzalez MC, Lu J, Jia G, Zheng J. Skeletal muscle mass and quality: evolution of modern measurement concepts in the context of sarcopenia. *Proc Nutr Soc*. 2015;74:355–366.
- Kullberg J, Brandberg J, Angelhed J-E, et al. Whole-body adipose tissue analysis: comparison of MRI, CT and dual energy x-ray absorptiometry. *Br J Radiol*. 2009;82:123–130.
- Deurenberg P, Weststrate KA, Seidell JC. Body mass index as a measure of body fatness: age- and sex-specific prediction formulas. *Br J Nutr*. 1991;65:105–114.
- James WPT, Waterlow JC; Obesity Research DHSS/MRC Group. *Research on Obesity: A Report of the DHSS/MRC Group*. London, U.K.: Her Majesty's Stationary Office; 1976. Publication 0114500347.
- Tahari AK, Chien D, Azadi JR, Wahl RL. Optimum lean body formulation for correction of standardized uptake value in PET imaging. *J Nucl Med*. 2014;55:1481–1484.
- Janmahasatian S, Dufull SB, Ash S, Ward LC, Byrne NM, Green B. Quantification of lean bodyweight. *Clin Pharmacokinet*. 2005;44:1051–1065.
- Erselcan T, Turgut B, Dogan D, Ozdemir S. Lean body mass-based standardized uptake value, derived from a predictive equation, might be misleading in PET studies. *Eur J Nucl Med Mol Imaging*. 2002;29:1630–1638.
- Chan T. Computerized method for automatic evaluation of lean body mass from PET/CT: comparison with predictive equations. *J Nucl Med*. 2012;53:130–137.
- Decazes P, Métivier D, Rouquette A, Talbot JN, Kerrou K. A method to improve the semiquantification of <sup>18</sup>F-FDG uptake: reliability of the estimated lean body mass using the conventional, low-dose CT from PET/CT. *J Nucl Med*. 2016;57:753–758.
- Kim CG, Kim WH, Kim MH, Kim D-W. Direct determination of lean body mass by CT in F-18 FDG PET/CT studies: comparison with estimates using predictive equations. *Nucl Med Mol Imaging*. 2013;47:98–103.
- Boellaard R, Delegado-Bolton R, Oyen WJG, et al. FDG PET/CT: EANM procedure guidelines for tumour imaging: version 2.0. *Eur J Nucl Med Mol Imaging*. 2015;42:328–354.
- Boellaard R, O'Doherty MJ, Weber WA, et al. FDG PET and PET/CT: EANM procedure guidelines for tumour PET imaging: version 1.0. *Eur J Nucl Med Mol Imaging*. 2010;37:181–200.
- Hamill JJ, Sunderland JJ, LeBlanc AK, Kojuma CJ, Wall J, Martin EB. Evaluation of CT-based lean-body SUV. *Med Phys*. 2013;40:092504.
- Bland JM, Altman DG. Statistical methods for assessing agreement between two methods of clinical measurement. *Lancet*. 1986;1:307–310.
- Lee J, Koh D, Ong CN. Statistical evaluation of agreement between two methods for measuring a quantitative variable. *Comput Biol Med*. 1989;19:61–70.